Highlights
20

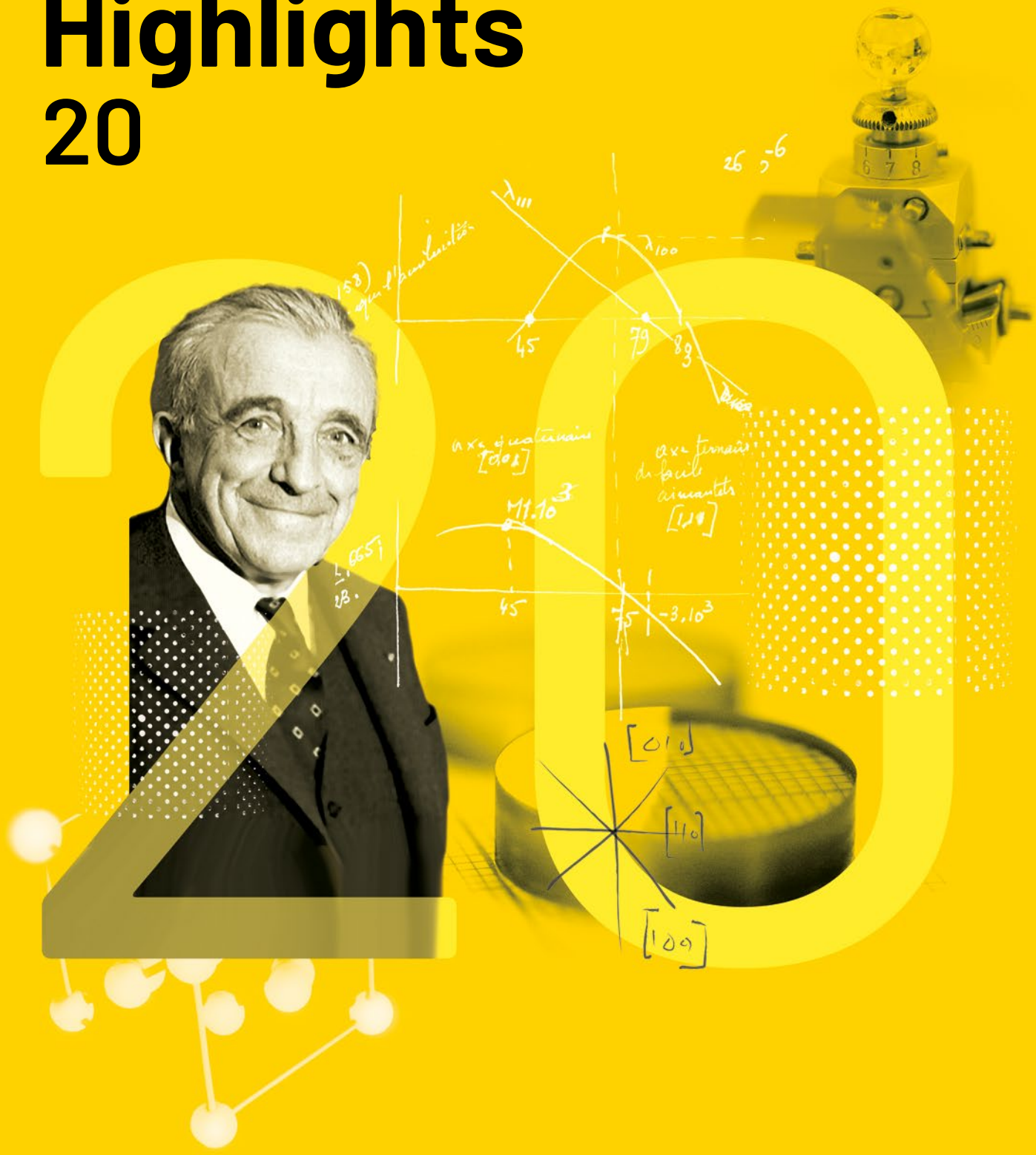

neel.cnrs.fr

NÉEL institut

Editorial

Welcome to this somewhat thinner-than-usual (but no less striking !) collection of the Institut Néel's scientific highlights !

Louis Néel received his Nobel prize exactly 50 years ago. Beside his seminal contributions to the theoretical understanding of magnetism, he had brought French and international science organisations to invest heavily here in Grenoble from the 1950's to the 1970's. He put Grenoble on the science and technology worldmap, attracting many international scientists and high-tech engineers.
As illustrated by the first two entries of this year's magazine, some among Louis Néel's scientific scions still explore magnetic phases, be it the intricate spin textures of frustrated magnets or a smectic phase in iron under pressures of geological-magnitude, a phase where superconductivity might coexist with magnetism. Also, in the spirit of their eminent forefather, other researchers have looked for ingenious applications of magnetism, illustrated here with magnetically-controlled sub-mm size robots.

Using scientific knowledge and in particular conceptual tools to tackle industrial challenges is another inherited trait, illustrated here in the energy-related fields of advanced catalysis, photovoltaics and ultraviolet light sources. In the latter case, exploiting nanowires has paved the way to viable deep-UV LED's. Even smaller nanowires were shown to be free of dislocations in highly strained but cleverly gradated hetero-juctions. Other semiconducting nanowires were observed to host "impossible" reversible chemical diffusion upon special annealing procedures. On another plane, a network of nanopores was used to demonstrate how fluids can evaporate from a "forest of nanotrees" by homogenous cavitation.

Finally, the gap between fabricating low-dimensional nanostructures and demonstrating quantum phenomena with a potential for application in solid state quantum technologies was overcome time and again at the Institut Néel in 2020, as illustrated by the local wave-mixing made possible by hybrid plasmonics, the non-invasive readout of superconducting Qubits, or the specific electronic topology observed on graphene heterostructures.

These are but a few of the scientific and technological accomplishments of the Institut Néel's personnel, despite the Covid-19 crisis that has made 2020 such a challenging year. I am sure that 2021 will bring many other achievements, under the guidance of my successor, Dr Laurence Magaud. I must thank all the Institute's personnel for their tenacity during this difficult year, and in particular the contributors to the present collection of articles. I would also like to acknowledge the constant trust of our institutional partners and in particular of both the CNRS and the Université Grenoble Alpes.

Finally, let me express my deep gratitude to Klaus, Laurence, Serge and Thierry, who have been a great team of Deputy Directors ! I wish the Institut Néel a bright and sustainable future, inspired by our predecessors and encouraged by our present successes.

Etienne Bustarret,
December 11, 2020
Grenoble, France

Contents

Spin texture
in a chiral magnet

Magnetic materials lie at the heart of information technology. Although research in this field has long favoured the use of ferromagnetic materials, growing interest has recently been turned to the possible advantageous use of "frustrated" antiferromagnets and of their "spin textures". In antiferromagnetic materials, the magnetic moments (the spins) of neighbouring atoms are anti-parallel to each other, so there is no overall magnetization. Their spin textures are modulations of the atomic magnetization over length scales from just a few atoms to hundreds of nanometres. Emblematic examples are magnetic helices and magnetic "skyrmions" (vortices of magnetic moments) and there is great interest in the physics governing their origin, as well as potential applications in emerging technologies. Additionally, in these spin textures, the magnetism might be coupled to motions of atoms or of electric charges, etc. Of particular interest are the so-called "multiferroics", materials where two different orderings, such as magnetism and ferroelectricity (i.e. spontaneous electric polarization) coexist and could be coupled to tailor various functionalities.

Here we report the direct observation of a novel kind of very long-wavelength spin modulation induced by applying a magnetic field in the antiferromagnetic compound Barium Tantalum Iron Silicate ($Ba_3TaFe_3Si_2O_{14}$). This compound, which has the trigonal langasite crystal structure, is characterized by the "chirality" of its crystallographic and magnetic structures. That is, it exists as left-handed and right-handed crystals ("chiral" comes from the Greek *kheir* for a "hand"). Fig. 1. displays the two chiral arrangements of the magnetic atoms, triangles of iron atoms lying in planes perpendicular to the crystal's trigonal axis c.

We have investigated $Ba_3TaFe_3Si_2O_{14}$ by combining experiments and theory in collaboration with the Interdisciplinary Research Institute of Grenoble, with a Swiss team and with a colleague at Groningen University. The langasite was studied by neutron diffraction at the Institut Laue Langevin (Grenoble) and at the Swiss Spallation Neutron Source, and by resonant X-ray diffraction at the BESSY II synchrotron (Germany). The specifically multiferroic properties were determined at the Institut Néel from the temperature and magnetic field dependence of the electric polarization.

In zero magnetic field, the spins (the magnetic moments) of all the crystal's iron atoms are at 120° from each other within the planes of triangles. In the perpendicular direction *c*, the spins are rotated progressively in successive planes, giving a spiral spin structure having opposite sense for left or right-handed crystal samples.

When we apply a magnetic field *H* greater than 4 Teslas perpendicular to the *c* axis, the spins rotate out of their planes, progressively along the *â* axis perpendicular to *c* (see Fig. 2). This is the field-induced spin texture, a spin-spiral perpendicular to the zero-field spiral. It is a new non-coplanar magnetic phase wavering between two helical states with perpendicular planes of rotation.

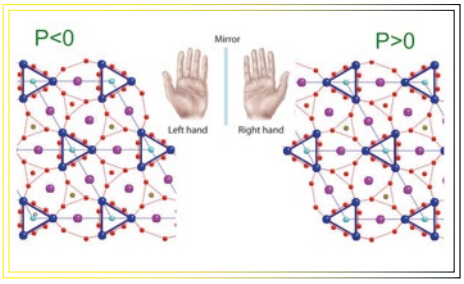

Fig. 1: Trigonal crystal structures of two $Ba_3TaFe_3Si_2O_{14}$ samples having left and right handed chirality. The magnetic Fe atoms (blue) are arranged in triangles in the a-b plane perpendicular to the trigonal axis c. The sign of the electric polarization P is chilarity dependent.

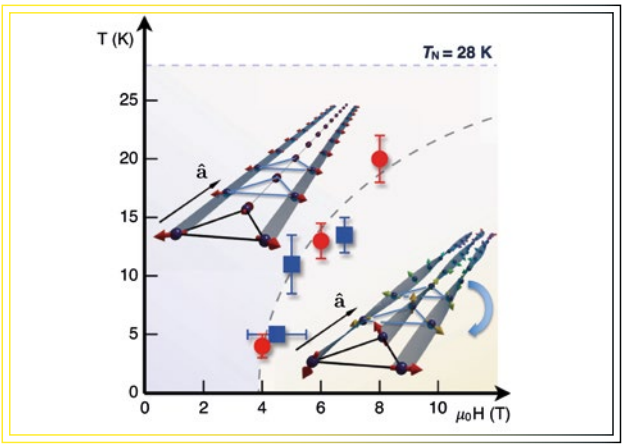

Fig. 2: Magnetic field vs temperature phase diagram of $Ba_3TaF_3Si_2O_{14}$. The spin texture phase is at right. Squares are from neutron and X-ray diffraction, circles are from electric polarization. Two diagrams show some Fe-atom triangles along the â axis perpendicular to the trigonal axis c. At left, all spins (red arrows) lie in plane a-b. At right, a field > 4 Teslas rotates the spins out of the a-b plane, progressively along â, creating a spiral spin texture over several hundred nm.

The most striking hallmark of this spin texture is the onset of a unique chirality-dependent contribution to the bulk electric polarization *P*. It changes sign for left handed and right handed samples. This makes $Ba_3TaFe_3Si_2O_{14}$ a magnetic field-induced multiferroic.

The length scale of the magnetic field-induced modulation is several hundreds of nm varying with *H*. We anticipate that novel exotic textures can be realized in other langasite-structure materials and in other non-centrosymmetric complex magnets, with additional multiferroic functionalities.

further reading...

• **Field-induced double spiral in a frustrated chiral magnet**
M. Ramakrishnan, E. Constable, A. Cano, M. Mostovoy, J.-S. White, N. Gurung, E. Schierle, S. de Brion, C.-V. Colin, F. Gay, P. Lejay, E. Ressouche, E. Weschke, V. Scagnoli, R. Ballou, V. Simonet & U. Staub
npj Quantum Materials 4, 60 (2019).

Contacts
andres.cano@neel.cnrs.fr • virginie.simonet@neel.cnrs.fr

Postdoc
Evan Constable

The mysterious magnetic phase of iron under high pressure unveiled

Iron and its alloys make up most of the core of rocky planets. So its study in the laboratory under extreme pressure and temperature sheds light on many aspects of planetary and earth science. Under ambient conditions iron crystallizes in a cubic lattice structure, but at pressures above 15 gigapascals (150 KBar), it transforms into a hexagonal structure called "εpsilon-iron". This change in the usual arrangement of atoms causes iron to lose its ferromagnetism, i.e. its magnetization due to a parallel alignment of atomic magnetic moments. It has been proposed that other forms of magnetism might remain under these high pressure conditions, but they had never been observed. Another intriguing aspect of ε-iron is that, at very low temperature (below 2 degrees Kelvin), it exhibits superconductivity. There have been suggestions that this could be an example of superconductivity induced by magnetic exchange excitations. But this would only be possible if some magnetism does exist in this range of very high pressure and very low temperature.

In order to investigate this possible magnetic state, we have worked with colleagues from the Institute of Mineralogy, Material Physics and Cosmochemistry (Paris), the SOLEIL synchrotron radiation source, and the Laue-Langevin Institute (ILL) in Grenoble. High pressure experiments were done with X-ray emission spectroscopy and neutron scattering. The results were interpreted using a Heisenberg model derived from first principles (Density Function Theory) and solved using classical Monte Carlo methods.

Neutron-diffraction studies of ε-iron done at the ILL, under record high pressure and low temperature conditions, found no signs of overall magnetic order, even though neutron diffraction is the best method for detecting long range magnetism. However, at SOLEIL, X-ray emission spectroscopy proved more probing. Analysis of X-Ray data accumulated over very long times to achieve unprecedented sensitivity showed that the electronic state of ε-iron is compatible with the presence of localized antiferromagnetic correlations without long-range order.

In fact, the theoretical modelling of the ε-iron system by Density Functional Theory had predicted the existence of an entirely new magnetic phase, which we call "a spin-smectic" state, see Fig. 1. In the smectic phase, the relative orientation and the absolute value of the magnetic moments (the spins of the iron atoms)

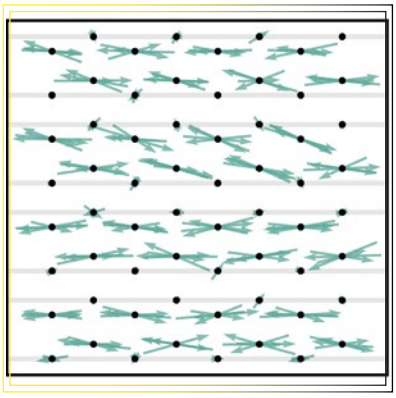

Fig. 1: Snapshot (viewed) perpendicular to the hexagonal c axis of the smectic phase of iron at low T, high pressure. Black dots represent the iron atoms. We are looking onto lines of iron atoms (hidden behind the front atom). The 6 arrows shown are the magnetic moments of 6 atoms seen at the same instant. This smectic state consists of organised antiferromagnetic bilayers (i.e. magnetic moments in two neighbouring-layers have opposite directions) but there are no magnetic correlations between the different bilayers. (The word «smectic» relates to the layered nature of common soap.)

fluctuate rapidly. This exotic magnetic state, where fluctuations would prevent the establishment of long-range magnetic order, can reconcile all the experimental observations on ε-iron. Thus, at low temperature, ε-iron has a non-zero but unordered magnetic moment, which gradually decreases with pressure and disappears beyond 30 gigapascals (see the phase diagram, Fig. 2). This range between 15 and 30 GPa covers the pressure range where ε-iron exhibits superconducting properties. So these properties could indeed be linked to magnetism at very low temperature. Remarkably, though magnetism of iron has been known since antiquity, this element's magnetic properties continue to captivate scientists to this day!

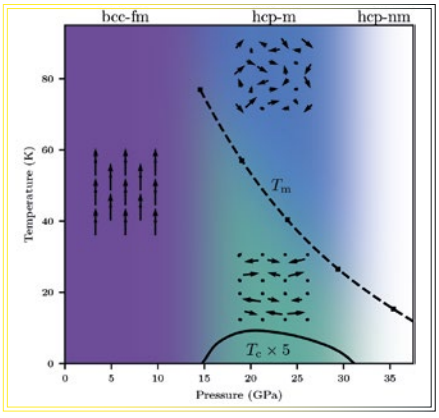

Fig. 2: Pressure vs Temperature phase diagram for iron. At left (low P) : the usual ferromagnetic α-iron cubic phase (bcc-fm, coloured purple). In the middle : under high pressure, epsilon-iron is in a hexagonal phase (hcp). At low temperature, below the curve T_m, epsilon-iron is in a magnetic smectic phase (green). (Above T_m , ε-iron is a completely disorganized spin liquide phase). Below the curve T_c , ε-iron is superconducting. The black arrows represent the magnetic moments of iron atoms in each phase.

further reading...

• **Epsilon iron as a spin-smectic state**
B.-W. Lebert, T. Gorni, M. Casula, S. Klotz, F. Baudelet, J.-M. Ablett, T.-C. Hansen, A. Juhin, A. Polian, P. Munsch, G. Le Marchand, Z. Zhang, J.-P. Rueff & M. d'Astuto
Proc. National Acad. Sci. 116, 20280 (2019).

Contact
matteo.dastuto@neel.cnrs.fr

Controlling micro-robots
with magnets

Micro-actuators or micro-robots are emerging tools that are particularly promising for life science applications. These applications can be in vitro (manipulation, mechanical stimulation, assembly) or in vivo (microsurgery, drug delivery, cell delivery). However, for micro-robots to be useful, we need to be able to control them remotely, in a confined environment, whether they are in locomotion or performing various actions. Magnetic actuation is ideal since an externally applied magnetic field can generate significant forces on a distant magnetic material, with minimal interaction with tissues or biological material. A micrometric actuator in which magnetic materials can be controlled in position and in magnetization direction is still particularly challenging below 1 mm.

In order to produce dexterous micro-robots at the 100 micron scale, we have collaborated with the Laboratoire Interdisciplinaire de Physique (Grenoble) to combine Neodymium-Iron-Boron (NdFeB) magnetic "microbeads" with structures fabricated by 2-photon polymerization. The latter is a "3D-micro-printing" technology providing sub-micrometer resolution which uses a focused green laser that polymerizes a UV-sensitive polymer photoresist locally, via a 2-photon absorption phenomenon. This technique allows fabrication of the flexible body of the micro-robot (yellow in Fig. 1).

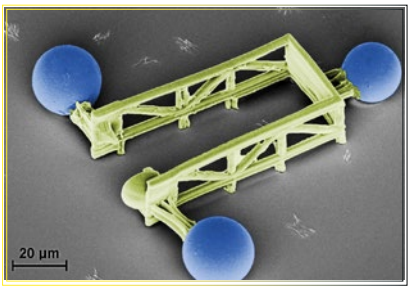

Fig. 1: Scanning electron micrograph of a magnetic micro-gripper (artificial colors). The robot's body (yellow) is made of a UV-curable polymer by micron scale 3D printing. The magnetic microbeads (in blue) are polycrystalline NdFeB.

The incorporation of the magnetic microbeads (blue in Fig. 1) requires a precise positioning and orientation of the magnetization of each individual bead. This task is performed thanks to an external magnetic field of variable direction, allowing the pre-magnetized bead to be rolled, positioned and oriented near the robot's body. The beads are then strongly attached to the structure by polymerizing a link between the body of the robot and each magnetic bead, and the remaining non-polymerized resist is rinsed away.

In Fig. 1, we show a micro-gripper for the manipulation of single cells. The distinct orientation of the magnetization of each bead (red arrows in Fig.2) is the key to the dexterous actuation of this micro-gripper. The opposing magnetization of the two beads on the gripper's arms cancel each other such that the remaining bead will align with an external magnetic field. A rotating magnetic field will then induce a rotation of the gripper, promoting rolling and thus translation. Application of a magnetic field gradient will generate a direct translation of the micro-gripper. Finally, an increased magnetic field applied along the gripper's long axis will align the arms' beads along the field, therefore opening the gripper's arms to grab a micrometric size object.
To improve the control over such micro-robots, a magnetic field generator (three nested Helmholtz coils) was fabricated in collaboration with Grenoble Electrical Engineering Lab (G2ELab), producing magnetic fields of controlled direction, magnitude and gradient. The combination of well-controlled magnetic materials and complex magnetic field sources will provide a new generation of multifunctional micro-robots particularly helpful for life sciences.

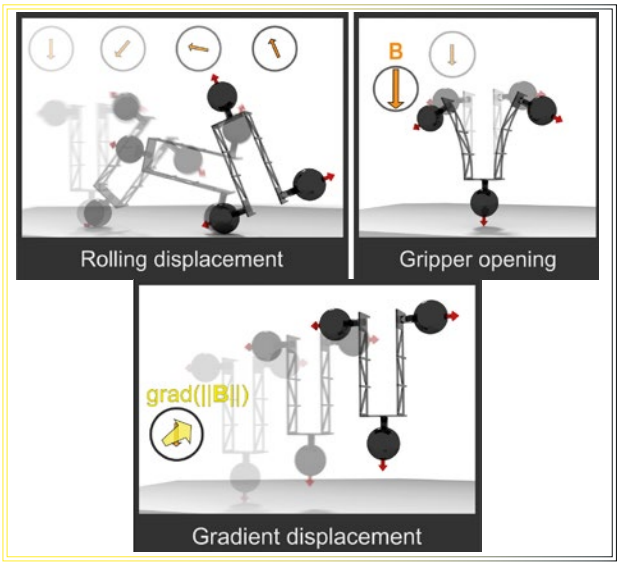

Fig. 2: Different actuation modes for the micro-gripper. At left : Under a rotating magnetic field, the gripper rotates and rolls on the substrate. In middle : increasing the magnetic field opens the gripper. At right : under a magnetic field gradient, the gripper translates towards high-field areas. Red arrows on the magnetic beads represent their direction of magnetization.

further reading...

• **Fabrication and Magnetic Actuation of 3D-Microprinted Multifunctional Hybrid Microstructures**
V. Vieille, R. Pétrot, O. Stephan, G. Delattre, F. Marchi, M. Verdier, O. Cugat & T. Devillers
Adv. Mater. Technol. 5 (2020), doi.org/10.1002/admt.202000535.

Contact
thibault.devillers@neel.cnrs.fr

PhD students
Victor Vieille • Roxane Pétrot

Towards better industrial catalysts
for reducing air pollution

Catalysts are materials that can promote chemical reactions. They can convert toxic components into non-toxic forms and play a fundamental role in cleaning up vehicle fuels. Nevertheless, optimization of industrial catalysts remains a challenge, mainly because they are relatively large multi-component bodies, consisting of active phases, supports, and additives. To better understand the relationships between their complex structure and their functionalities, it is crucial to characterize their inner structure with high resolution and high sensitivity. This also allows detection of defects or unexpected deposits of harmful materials, which can develop in a catalyst's structure during operation, thereby reducing its lifetime. For this purpose, we are developing Ptychographic X-ray Computed Tomography (PXCT), an emerging, non-destructive, 3D X-ray microscopy technique, which is revolutionizing the characterization of industrial catalysts.

The removal of sulphur from crude oil by hydro-desulphurization (HDS) is an essential catalytic process in the petroleum industry. It ensures production of clean refined-petroleum products, such as diesel, kerosene, and jet fuel. Especially It allows creation of ultra-low-sulphur diesel, which is critical to reducing the toxic sulphur dioxide (SO_2) emitted by trucks as well as automobiles.
To remove sulphur, the petroleum gas is forced under high pressure and high temperature through a support matrix, a highly porous material alumina (γ–Al_2O_3) that provides a very large interior surface area to carry the catalyst, the transition metals Molybdenum (Mo) and Nickel (Ni), which forms slabs of "NiMo". However, the effectiveness of this procedure depends on the microstructure of the HDS catalysts used in the oil refinery, which determines the accessibility of reactants to the active catalyst sites on the interior of the porous matrix.
Characterization of this microstructure is needed to differentiate the various zones of the sample. We have used Ptychographic X-Ray Computed Topography (PXCT) to characterize a series of HDS catalysts, at the Swiss synchrotron (the Swiss Light Source). PXCT combines ptychography (from the Greek: πτηξ= fold and: γραφη= writing) and computed tomography to obtain 3D imaging of the microstructure of our materials. In ptychography, the sample is scanned by a spatially-restricted highly coherent X-ray beam across a grid of partially overlapping target spots. This allows retrieving the phase shifts using advanced algorithms and enables us to achieve nanoscale spatial resolution independent of the X-Ray probe size. In PXCT, a ptychography experiment is repeated at each angle over 180 degrees-rotation of the sample. Afterwards, the phase-retrieved 2D images are combined into tomographic reconstruction algorithms to yield 3D images. We achieved a spatial resolution of about 50 nm with a voxel (volume pixel) size of 30 nm.
By probing the inner microstructure of an industrial alumina carrier: unloaded, loaded with a Mo catalyst, and loaded with both Mo and Ni catalysts, we obtained a wide range of valuable information about the carrier's porous structure and the distribution of the catalysts. Especially, and surprisingly, this work revealed a build of the alumina carrier consisting of two interwoven phases of the alumina matrix differing in the size of their nanopores regardless of the catalyst loading.
This first-time observation of a two-phase build of the alumina carrier has the potential to deepen our understanding of a wide range of hydroprocessing catalysts. Our results should enable further calculations of reactant diffusivities in the carrier's pores, and guide manufacturing methods to obtain a better distribution of the NiMo active phase in next-generation HDS catalysts.

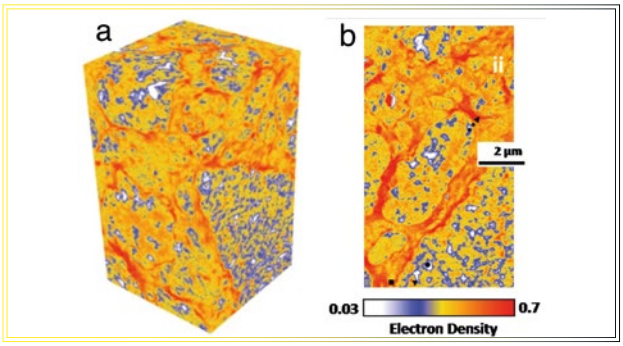

Fig. 1: (a) A region of a 3D image, obtained by PXCT, of the electron density inside a sample of a Nickel-Molybdenum hydro-desulphurization catalyst. (b) A 2D image, which is a vertical cut through the electron-density volume of (a).
The Ni-Mo catalyst lies inside the nanoscale pores of an Al_2O_3 support material. The colour scale-bar represents the electron density in units of electrons per angstrom cubed. These colours correspond to the fraction of air, Al_2O_3 support and Ni-Mo catalyst in each 30 nm «voxel» (3D pixel). The less dense, most porous material, which contains much air, appears towards white, while the densest alumina and catalyst materials appear closer to red.

further reading...

• **Hierarchical Structure of NiMo Hydrodesulfurization Catalysts Determined by Ptychographic X-ray Computed Tomography**
J. Ihli, L. Bloch, F. Krumeich, K. Wakonig, M. Holler, M. Guizar-Sicairos, T. Weber, J.-C. da Silva, & J.-A. van Bokhoven
Angew. Chem. Int. 59, 17266 (2020).

Contact
julio-cesar.da-silva@neel.cnrs.fr

Why are halide perovskites so efficient for solar cells?

Recently, a new class of photovoltaic materials has appeared, the halide perovskites, which promise efficient solar cells at low cost. These materials with the perovskite crystal-structure are made of abundant constituents and can be produced by soft-chemistry processes. They are attracting tremendous attention and already show very good photovoltaic conversion efficiency with low-cost technology. But the halide perovskites are complex materials and fundamental understanding of the basic physical processes involved in the photovoltaic conversion is needed. In a recent theoretical study, we have analyzed the electronic structure and transport properties of "$MAPbI_3$" (Methyl-Ammonium Lead Iodide), the principal halide perovskite material for solar cells.

In a perovskite-based solar cell, light is absorbed in the central part, the perovskite material. The perovskite is an excellent absorber and one micron thickness is enough to absorb all the incident photons of energy greater than the bandgap energy. Then the electrons and the holes produced by the absorption of photons diffuse sufficiently quickly and have sufficiently long lifetimes so that they can reach their respective metal contacts before they can recombine with each other. Thus the perovskite combines three essential electronic characteristics for efficient solar cells, namely high light absorbance, sufficient charge-carrier mobility and long carrier lifetime. Understanding the origin of these good properties is a major theoretical challenge.

In collaboration with G. Trambly de Laissardière of Cergy Paris University, we analysed theoretically the electronic transport properties of the $MAPbI_3$ perovskite crystal. We calculated that the mobilities of the intrinsic material are about 80 cm^2/Vs and we showed that quantum localization effects, which had never been considered, are very important.
When there is additional extrinsic disorder with mobilities below about 30 cm^2/Vs we propose that a new type of transport regime occurs that we call adiabatic quantum localization. This regime is a novel type of electronic transport and differs fundamentally from the two standard regimes that are electronic band-like conduction and thermally-activated hopping conduction. In this non-standard regime the charge carriers have enough time to reach a localized state before the atoms move. Yet they can diffuse because their localized state constantly adapts itself to the motion of the atoms. A similar regime has been proposed recently for organic semi-conductors by Institut Néel and Italian collegues.

Our study shows that the thermal displacements of Lead and Iodine ions generate a large electrical potential equal to about half the perovskite's 1.6 eV bandgap. As shown in Fig. 1, the displacements generate zones of positive or negative potential at the scale of a few unit cells of the cubic crystal. This potential plays an essential role for promoting the electronic mobilities. We believe that it could also have a strong impact on the recombination lifetime or even on the ionic diffusion which is known to play an important role for perovskite-based solar cells.

In summary, we find that large fluctuations of the inner electrical potential play a key role for the electronic mobilities in this solar-cell material, and they could also have a central role for other electrical properties such as electron-hole recombination.

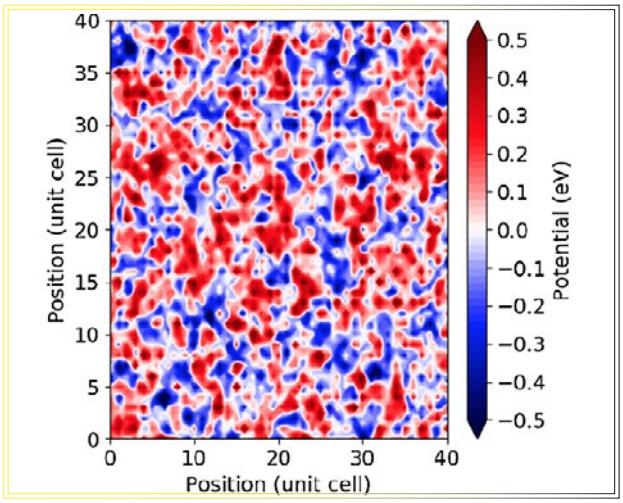

Fig. 1: Instantaneous electrical potential inside the $MAPbI_3$ perovskite. The potential fluctuates in space over typically a few unit cells i.e. over 1 to 2 nm. The amplitude of this variation is of order 0.5 eV to 1 eV (see the colour bar), which is about half the band gap. The potential fluctuates with time due to thermal motion of the Pb and Iodine atoms.

further reading...

- **Modeling of Electronic Mobilities in Halide Perovskites: Adiabatic Quantum Localization Scenario**
  A. Lacroix, G. Trambly de Laissardière, P. Quémerais, J.-P. Julien & D. Mayou.
  Phys. Rev. Lett. 124, 196601 (2020).
- **A Map of High-Mobility Molecular Semi-Conductors**
  S. Fratini, S. Ciuchi, D. Mayou, G. Trambly de Laissardière & A.Troisi. *Nat. Mater.* 16, 998 (2017).

Contacts
jean-pierre.julien@neel.cnrs.fr • didier.mayou@neel.cnrs.fr

PhD student
Antoine Lacroix

Aluminium Nitride nanowires:
towards efficient deep-ultraviolet LEDs

The recent emergence of Covid-19 and the likelihood of other emerging pathogens make it particularly urgent to find effective and easy-to-use solutions for surface disinfection and water purification. To sterilize a surface or water, deep-UV light, below 280 nm, is required. For decades, mercury-vapour lamps have been used for such purposes. However, due to the hazards of mercury, mercury lamps are progressively being banned world-wide. This should boost the rapidly growing market for deep-UV Light Emitting Diodes (LEDs). However, their poor p-type electrical conductivity drastically reduces their efficiency. Improving the p-type conductivity is thus a major challenge.

These deep-UV light-emitting diodes are made from nitrides of group III semiconductors, specifically aluminium nitride (AlN), alloyed with some gallium nitride (GaN). In these devices, when an electrical bias voltage is applied, an electron (negatively charged) and a hole (positively charged) annihilate each other in the "active region" emitting a UV photon. But until now deep-UV LEDs have remained in the lab because of their very low optoelectronic efficiency. So, several technological obstacles have to be overcome.
Especially, one of the main challenge is that, for the AlN alloys that emit deep-UV light, there has been no good p-type material to conduct holes efficiently to the active region. Effective "p-doping" requires introducing magnesium (Mg) acceptor atoms to provide free holes. In existing deep-UV LEDs, not enough Mg could be incorporated into the AlN material.
In this context, in collaboration with colleagues from the CEA's Institut de Recherche Interdisciplinaire de Grenoble, we have been using plasma-assisted Molecular Beam Epitaxy to grow AlN materials in the form of densely packed, 100 nm diameter "nanowires", see Fig. 1. The advantage, compared to conventional planar diode structures, is that these "long and thin" objects contain no deleterious dislocation defects. We have investigated the MBE growth conditions for achieving efficient Mg p-doping in these nanowires. Especially, supported by *ab-initio* theoretical calculations of the effects of dopant atoms in nitride crystal lattices, we obtain better incorporation of magnesium in AlN nanowires if we simultaneously incorporate a small fraction of Indium (In) atoms.

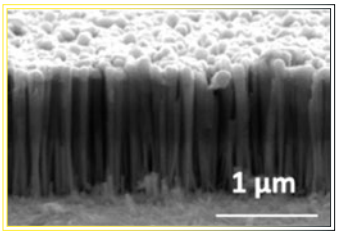

Fig. 1: Scanning Electron Microscope image of densely packed $Al_{1-x}Ga_xN$ crystalline nanowires on a conducting silicon substrate. The amorphous layer seen on top of the nanowires is Indium Tin Oxide (ITO), which provides an ohmic contact.

Our nanowires were metalized at Nanofab, the Institut Néel's clean-room facility, to create prototype p-i-n diode devices (see Fig.2). To study the *p*-type conduction in the Mg-Indium co-doped segments of the nanowire diodes, we measured the electrical current induced by a tightly focussed, scanning electron beam (Fig. 2) to precisely locate and characterize the p-i-n junctions with a spatial resolution better than 50 nm.
Unexpectedly, we discovered that electron-beam irradiation can further improve the electrical activation of the Mg dopant by five orders of magnitude, an effect not yet properly understood. Finally, optical characterization of our diodes shows electroluminescence in a broad band in the deep-UV.
Our process, exploiting the excellent properties of nitride nanowires, has been patented and paves the way for realization of a new class of efficient deep-Ultraviolet LEDs.

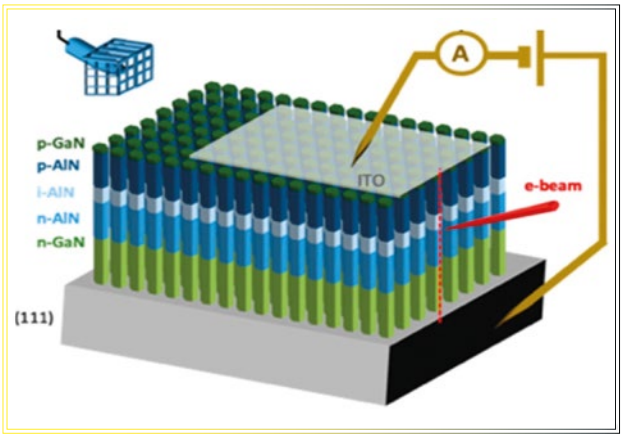

Fig. 2: Structure of an AlN alloy p-i-n junction LED. Holes from Mg doped p-AlN nanowire segments and electrons from Silicon donor-doped n-type AlN segments annihilate in short insulating (i-AlN) segments. Electrical contacts to the diode are made between the silicon substrate and the transparent Indium Tin Oxide top layer.

further reading...

• **Mg and In codoped p-type AlN nanowires for pn junction realization**
A.-M. Siladie, G. Jacopin, A. Cros, N. Garro, E. Robin, D. Caliste, P. Pochet, F. Donatini, J. Pernot & B. Daudin
Nano Lett. 19, 8357 (2019).

Contacts
gwenole.jacopin@neel.cnrs.fr • julien.pernot@neel.cnrs.fr

PhD student
Alexandra-Madalina Siladie

Tweaking strain
at nanowire interfaces

Some of the toughest substances in the world are crystals, in which planes of atoms arrange themselves in lattices held together by chemical bonds. Deforming a crystal is hard without breaking some bonds. This degrades the performance of materials, be it for sturdiness such as in a bridge. It is also true at the microscale, as the performance of a laser or a computer chip rely on how light or electrical current will be perturbed by defects created in a crystal. Interfacing two crystals by forming a "heterostructure" has been of high interest over the past 60 years, as it is fundamental to many novel electronic devices. Different crystals have different lattices and a natural way to compensate for this mismatch is for the materials to compress and expand at the interface, creating a mechanically strained region. But this is also a recipe for introducing defects called dislocations.

In collaboration with colleagues at the CEA's Interdisciplinary Research Institute of Grenoble, and with the Centre for Nanoscience and Nanotechnology (Palaiseau) and the Eindhoven University of Technology (The Netherlands), Institut Néel researchers have developed a solution to create an interface between two crystals which ensures that no dislocations are formed. This work involves nanowire heterostructures grown on silicon substrates formed by the successive growth of two materials along the nanowire axis. These objects are wire-shaped crystals smaller than a thousandth of the thickness of a human hair. In a nanowire there are relatively few atoms in the cross-section, therefore, it is easier for the lattice to deform elastically. Two different materials can be easily combined even if their lattice parameters differ by several percent. Nevertheless, excessive mechanical strain is not recommended, as it would strongly influence the electronic properties of the interface.
Remarkably, we obtain a stress reduction of 75% in the case of a gradated interface of 5 nm nanometers between two greatly mismatched crystals: $In_{0.8}Ga_{0.2}As$ and GaAs (6% lattice parameter difference). The gradated interface is formed by an alloy whose composition $In_{1-x}Ga_xAs$ gradually varies from one material to the other. Such gradated interfaces are made possible via the control of the fluxes, i.e. the number of atoms arriving at the surface during the growth of the nanowires by Molecular Beam Epitaxy. In this situation, the challenge is to prevent the formation of kinks along the nanowire by a careful adjustment of all the growth parameters: the flux of each species, the different growth temperatures and the growth interruptions.
We performed chemical and structural characterizations of the interface by combining energy dispersive X-ray spectroscopy and high-resolution Transmission Electron Microscopy. The crystal lattice at the interface is continuous without dislocations, and the deformation due to the large mismatch is clearly visible on the electron microscope images (Fig. 1). These experimental results are in excellent agreement with Finite Element Calculations.
With a gradated interface of only 5 nm length, we confirm a very strong reduction in mechanical stress, down to almost zero % at the junction between these two technologically important semiconductors InGaAs and GaAs. Finally, this work increases the possibilities for the design of nanowire heterostructures: not only the material composition in each segment of the structure can be selected but also the composition of the interface. It shows the growing importance of interfaces in the design of nanomaterials for integrated optoelectronics and photonics on silicon.

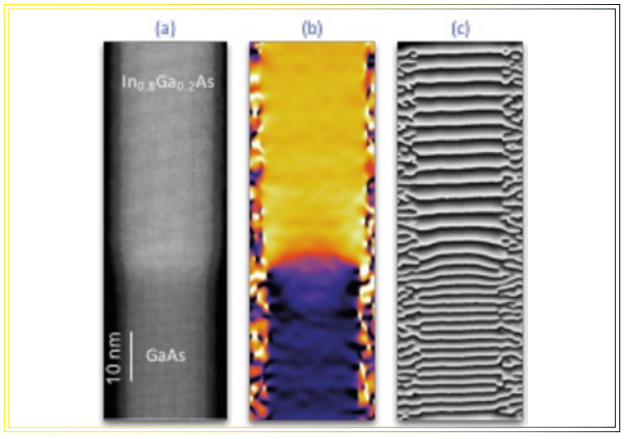

Fig. 1 : Images showing the interface region in an $In_{0.8}Ga_{0.2}As$-on-GaAs nanowire heterojunction. The nanowire diameter is 20 nm. (a) Transmission Electron Microscopy image with atomic resolution. (b) Coloured image showing the different lattice parameters obtained by geometrical phase analysis of this microscope image and (c) corresponding Moiré pattern highlighting the deformation of the lattice planes due to the ~6 % lattice-parameter mismatch between GaAs and $In_{0.8}Ga_{0.2}As$. Elastic deformation takes place along the sidewalls of the nanowire in the interface region, whereas the nanowire core remains under stress.

further reading...

- **Dislocation-free axial InAs-on-GaAs nanowires on silicon**
  D.-V. Beznasyuk, E. Robin, M. Den Hertog, J. Claudon & M. Hocevar. *Nanotech*. 28, 365602 (2017).
- **Full characterization and modeling of graded interfaces in a high lattice-mismatch axial nanowire heterostructure**
  D.-V. Beznasyuk, P. Stepanov, J.-L. Rouvière, F. Glas, M. Verheijen, J. Claudon & M. Hocevar
  Phys. Rev. Materials 4, 074607 (2020).

Contact
moira.hocevar@neel.cnrs.fr

PhD student
Daria Beznasyuk

Reversible diffusion of
aluminium and silicon atoms in a nanowire

Diffusion is a phenomenon whereby matter is transported from a region with high concentration to a region with lower concentration. We all know its effect: If I open the window on a cold day, the inside and outside temperatures will slowly converge since fast and hot gas molecules from inside mingle with the slower and colder gas molecules from outside. We also know that we cannot reverse this effect and "unmix" the hot and cold molecules, we cannot command the hot molecules to come back inside! But in a specific solid-state system, we can do exactly this.

This reversible diffusion phenomenon was an accidental observation during research on making electrical contacts on semiconductor nanowires. A nanowire is a thin, wire-like structure, of diameter several nanometres to tens of nanometres. Nanowires fabricated from semiconducting materials can be used in devices such as field-effect transistors, light-emitting diodes and solar cells. Nanowires incorporate insertions of different materials but, in devices, they require high-quality electrical contacts.

With colleagues at the Institute for Interdisciplinary Research of Grenoble we have been fabricating aluminium contacts onto Silicon-Germanium (Si-Ge) alloy nanowires. For an electron microscopy study of this process, Al contact-pads were fabricated on a $Si_{0.67}Ge_{0.33}$ nanowire positioned on a thin SiN membrane transparent to the very fast electrons of a scanning Transmission Electron Microscope (TEM). These structures were then heated inside the TEM, to image the solid-state reactions with nanometre resolution.

At 580°C, a solid-state reaction is started where the aluminium from the metal contact pad diffuses progressively into the nanowire, replacing germanium and silicon atoms. The Ge and Si atoms diffuse in the opposite direction, along the nanowire surface, exit the nanowire, and incorporate at surfaces and grain boundaries in the aluminium pad. Thus, a near perfect monocrystalline aluminium nanowire section is formed, with a perfectly abrupt interface to the SiGe nanowire, and making excellent electrical contact with it, see Fig. 1 (top).

Surprisingly, if the heating temperature is lowered very slowly, the Al contacts can no longer contain all the silicon atoms they had stored. The Si atoms (and also, but much less, the heavier Ge atoms) diffuse back along the nanowire and nucleate at the Al/SiGe interface, progressively forming a region of almost pure Si, with a low Ge content. This region grows in the reverse direction as the Al atoms return to the metal pad (Fig. 1, bottom).

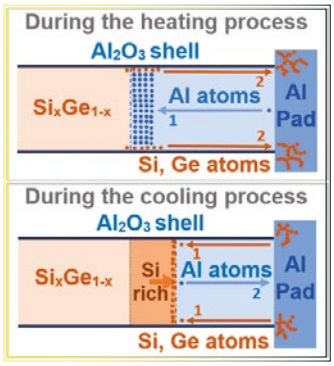

Fig. 1: At top: Diffusion of aluminium into the $Si_{0.67}Ge_{0.33}$ alloy nanowire, and diffusion of silicon and germanium out into the Al contact pad. Below: The reverse diffusion process for Al and Si ; the lesser reversibility for Ge diffusion produces a Si-rich region.

We found that the aluminium could move in and out repeatedly. To our knowledge, this work demonstrates a reversible diffusion mechanism for the first time, and absolutely unambiguously, thanks to the in-situ Electron Microscopy experiments. The reversible diffusion arises due to the nanowire geometry and crystallinity. This concept may be extended to other material systems. In our own work, the different diffusion properties of Si and Ge have allowed us to fabricate and contact complex and abrupt Al metal/Si-rich/SiGe alloy heterostructures with sharp interfaces in a single processing step, all compatible with current Si/Ge technology, see Fig. 2.

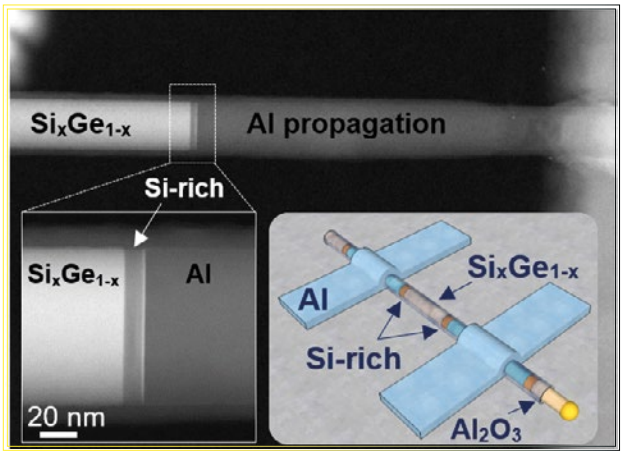

Fig. 2: At top: Scanning Transmission Electron Microscopy image of a nanowire heterostructure encapsulated in an Al_2O_3 shell. Below left: A zoom onto the SiGe alloy/Si-rich alloy/Al metal contact. At bottom right: a nanowire double-heterojunction structure.

further reading...

• **Reversible Al Propagation in Si_xGe_{1-x} Nanowires: Implications for Electrical Contact Formation**
M.-A.Luong, E. Robin, N. Pauc, P. Gentile, T. Baron, B. Salem, M. Sistani, A. Lugstein, M. Spies, B. Fernandez, & M. den Hertog
ACS Appl. Nano Mater. 3, 10, 10427 (2020).

Contact
martien.den-hertog@neel.cnrs.fr

PhD student
Minh Anh Luong (Institut Néel & IRIG)

Cavitation in a forest
of artificial nanotrees

Pull slightly on a solid. It will expand, and, when released, it will contract back to its original size just as a spring does. Pull harder, and the solid will break. Surprisingly, the same holds true for a liquid. Attractive interactions between the liquid's molecules allow the liquid to resist a pulling stress, up to an ultimate tensile strength beyond which the liquid "breaks" and a vapour bubble spontaneously appears. This phenomenon, called "cavitation", can be observed often, for example in the wake from a boat's propellers or the rise of sap in trees.

Due to the energy cost of forming an interface between liquid and vapour, the creation of a bubble in a bulk liquid is expected to be a thermally activated process described by the homogeneous Classical Nucleation Theory. This theory has been checked in experiments where the liquid is alternately compressed and stretched by a focused high-frequency ultrasonic pressure wave.
An alternative, quasi-static method to stretch the liquid has been devised recently in order to understand how cavitation affects the ascent of sap in trees, a phenomenon which is driven by the transpiration of the tree's foliage. The idea of the so called "artificial-tree" method is to enclose the liquid in a macroscopic cavity separated from a vapour reservoir by a porous plug allowing the exchange of matter between the vapour and the liquid.
Due to the resulting equality of chemical potentials between the vapour and the liquid, decreasing the external reservoir's pressure below the saturated vapour pressure stretches the liquid inside the cavity, allowing it to reach extremely negative pressures. By this same mechanism, negative pressures are obtained within the ducts of tree leaves, providing pumping of sap from the ground level up to considerable heights (up to 100 m in giant sequoia trees).
Our work relies on the same idea but, instead of a single macroscopic cavity, we study assemblies of billions of nanometre-sized pores etched in a membrane (see Fig. 1). Each tiny pore consists in a cavity coupled to the single large vapour reservoir through a narrower constriction. As with the porous-plug method mentioned above, the constrictions are narrow enough to stabilize the liquid inside the membrane, thus blocking the process of evaporation from the membrane's surface, allowing us to observe cavitation-driven evaporation in the cavities (Fig. 2).

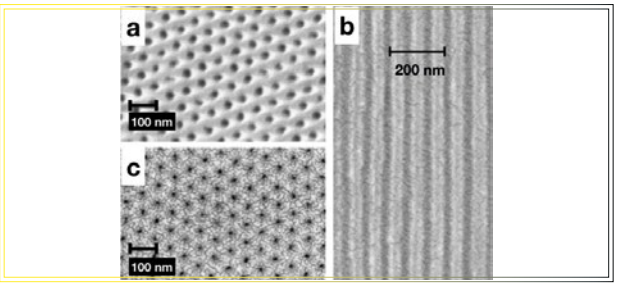

Fig. 1: Scanning Electron Microscope images of samples used for obtaining and observing cavitation in a forest of «artificial nanotrees». We start from a porous alumina (Al_2O_3) membrane, with long parallel cylindrical nanopores of 30 nm diameter and length 100 microns, obtained by a self-organization process. Image (a) is a top view, (b) is a side view. Then we deposit alumina at the open mouths of the pores, forming the constrictions seen in image (c).

The liquid used in our study is hexane (C_6H_{14}). For a fixed pressure in the vapour reservoir, we study the cavitation statistics by optical monitoring of the time decay of the fraction of filled pores. We find that the cavitation rate increases from totally negligible to a large value within a very narrow interval around a negative liquid pressure of -200 bar. Both the absolute decay rate and its pressure dependence are found to be quite close to the predictions of the Classical Nucleation Theory.
This confirms the latter theory, and our results definitively establish homogeneous cavitation as an important evaporation mechanism in nanoporous materials.
Beyond these results, our experimental system opens new prospects for fundamental studies of cavitation, and for the study of liquids in deeply metastable states. In particular, together with our partners at the Institut des Nanosciences de Paris and the Laboratoire de Physique de l'Ecole Normale Supérieure, Paris, we will seek to reduce the cavity radius below 10 nm to study the influence of an extreme nanoconfinement on cavitation.

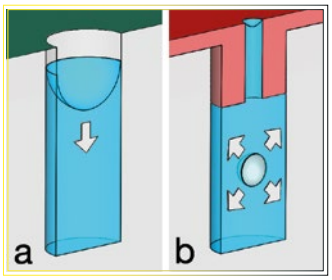

Fig. 2: At left : A pore (radius of order 30 nm) is completely open to the vapour reservoir. The liquid in the pore can evaporate completely via recession of the concave liquid-vapour meniscus.
At right : With a constriction smaller than about 5 nm in diameter, recession of the meniscus is blocked. The liquid in the cavity then evaporates by a cavitation process : A gas bubble nucleates spontaneously and then expands, pushing the surrounding liquid out through the constriction.

further reading...

• **Direct observation of homogeneous cavitation in nanopores**
V. Doebele, A. Benoit-Gonin, F. Souris, L. Cagnon, P. Spathis, P.-E. Wolf, A. Grosman, M. Bossert, I. Trimaille, C. Noûs & E. Rolley
Phys. Rev. Lett. 125, 255701 (2020).

Contacts
pierre-etienne.wolf@neel.cnrs.fr • panayotis.spathis@neel.cnrs.fr
laurent.cagnon@neel.cnrs.fr

PhD student
Victor Doebele

Wave-mixing at the nanoscale
with hybrid nonlinear plasmonics

Quantum technology is undergoing its second revolution by fully exploiting the wave-nature of quantum states, including the key roles played by their phase, their superposition and their entanglement. This is foreseen to foster applications that will strongly impact the future. The challenges are numerous in this quest, but on-chip integration of optical components remains a real bottleneck. Specifically, integration of ultimate optical sources involves all steps from generation of single photons to their detection, including their manipulation with optical circuits. In this context, our project focuses on photon generation with the ambition of establishing new roads toward emission of entangled photons from nanometre-scale light sources.

In this work, we take advantage of the strong optical nonlinearity of Potassium Titanyl Phosphate ("KTP") nanocrystals. We enhance the optical field of a single nanocrystal of KTP using plasmonic antennas, which boost the efficiency of light-wave mixing by up to three orders of magnitude as compared to a bare KTP nanocrystal. Using Finite Elements Methods for designing optimal physical structures, we developed nano-fabrication techniques for inserting a nanocrystal in a metallic plasmonic antenna, and we performed nonlinear optical measurements at the single photon level. The implications of this new "nano-platform" are numerous, especially in view of creating photon-pair sources at the nanoscale, beating the diffraction limit by construction. Our recent achievements concern the coupling of a nonlinear light emitter, a KTP nanocrystal, to plasmonic "nano-antennas" whose resonances localize and magnify the amplitude of the electric field. The evanescent nature of the near-field surrounding the antennas requires positioning the nanocrystal with nanometre resolution. This was possible thanks to the electron-beam masker at the Institut Néel's "Nano-Fab" technology platform. It allowed us to build hybrid nanostructures through a "top-down" approach. We first selected a good nanocrystal candidate based on polarization-resolved measurements of its Second Harmonic Generation properties (a nonlinear process where two photons are converted into a single photon of doubled energy). Then, two plasmonics structures were fabricated around the nanocrystal by electron-beam lithography, laying it centred in the gap between two antennas.

Best antenna geometries were determined on the basis of numerical simulations describing the complete experimental configuration (i.e. the focusing by a high numerical aperture microscope objective onto a single nanostructure, presence of the substrate, etc.). The simulations were used to optimize the dimensions of both gold and aluminium nano-antennas, in order to tune their plasmonic resonance-frequency to the photons involved in the process. Importantly, the simulations have provided quantitative predictions of the enhancements. The measured nonlinear response of this nanocrystal + antenna structure is enhanced by up to three orders of magnitude. Fig. 1 shows some typical results.

The next step in this work will be to switch from Second Harmonic Generation to photon-pair generation (the reverse process), which is at the core of many quantum-technology applications. We have already developed quantum simulations in this prospect and have shown the experimental feasibility. In view of the faint signals that are anticipated, this proof of concept is a major challenge that we want to take up!

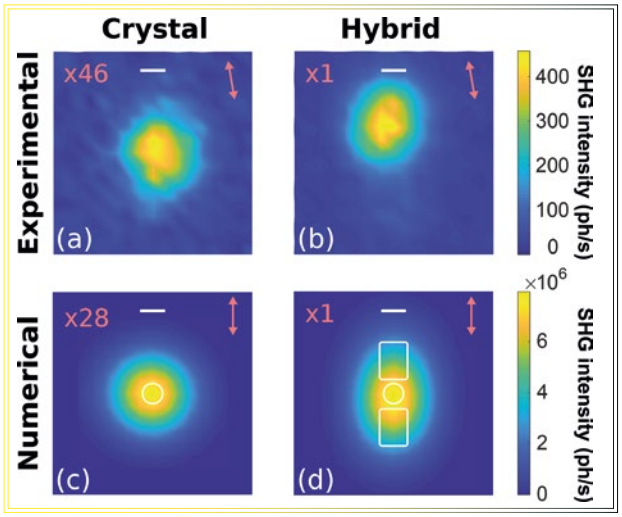

Fig. 1: Optical microscopy maps of the intensity of Second Harmonic light emission at 425 nm from a bare KTP crystal (at left), and from the hybrid structure which consists of the crystal inserted in the plasmonics-antenna gap (at right). Panels (a) and (b) are experimental data, (c) and (d) are predictions from simulations. Colours correspond to photon-counts per second. The white scale bars' lengths are 100 nm.
Normalization factors (x 46, etc.) for the light intensities are indicated on each panel. (The normalization factor differs between simulated and measured data are due to optical elements transmission-coefficients and detector efficiencies).

further reading...

• **Hybrid KTP-plasmonic nanostructures for enhanced nonlinear optics at the nanoscale**
N. Chauvet, M. Ethis de Corny, M. Jeannin, G. Laurent, S. Huant, T. Gacoin, G. Dantelle, G. Nogues & G. Bachelier
ACS Photonics, 7, 665 (2020).

Contacts
guillaume.bachelier@neel.cnrs.fr • gilles.nogues@neel.cnrs.fr
geraldine.dantelle@neel.cnrs.fr

PhD students
Nicolas Chauvet • Maeliss Ethis de Corny
Guillaume Laurent

Measuring a superconducting quantum bit

The measurement of any quantum system presents a fundamental contradiction: to verify its quantum properties the system must be isolated from the outside, classical world. But, oppositely, measurement is only possible when the system is connected to the outside world. We have been studying this contradiction in a quantum system consisting of a superconducting quantum bit (a "qubit") coupled to a radiative microwave field which carries the information to a classical detector. The superconducting qubit itself is realized by a superconducting nonlinear LC circuit oscillating at microwave frequency ν_q = 5 GHz. The two states of the qubit, $|g\rangle$ and $|e\rangle$, correspond to the ground and first excited state of this oscillator whose energy difference is given by an energy quantum $h\nu_q$, where h is Planck's constant. The qubit is inserted in a copper microwave cavity having two openings of the microwave field to the outside world.

Until now, the coupling between the qubit and the microwave radiation field has been done by energy exchange between the qubit and the cavity. Such a coupling is intrinsically destructive with respect to the qubit since it disturbs the qubit's state. In our experiment, we have developed a new coupling called "Cross-Kerr". This induces a shift of the microwave cavity's resonance frequency ν, dependent on whether the qubit is in the state $|g\rangle$ or $|e\rangle$. We apply a microwave field at the entrance of the cavity and we measure the transmitted microwave amplitudes, which depend strongly on the qubit's state. With care, this coupling can provide a non-destructive measurement of the qubit.

The qubit itself (Fig. 1) is realized by an aluminium superconducting circuit containing two Josephson tunnel junctions of submicron size. Electron-beam lithography was used to create a resin mask employed for defining the microwave circuit during thin-film evaporation of the aluminium. The superconducting properties of the circuit are essential for obtaining a non-dissipative microwave oscillator with quality factors as large as 100 000. In order that thermally-induced fluctuations do not mix the two quantum states, the experiments must be performed at $k_B T << h\nu_q$. The oscillator is held at the very low temperature of 30 mK in a dilution cryostat designed and built at the Institut Néel.

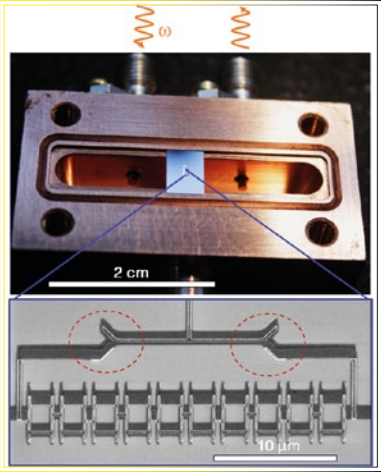

Fig. 1: (a) An aluminium superconductor quantum circuit on its silicon substrate is inserted in the centre of a 7 GHz copper microwave cavity. The two oscillating arrows ω represent the incoming and transmitted microwave signal. (b) The zoom is a Scanning Electron Microscope image of the superconducting circuit. The two red circles indicate the two small tunnel junctions.

Measuring the signal transmitted by the cavity may disturb the state of the qubit. So the microwave energy in the cavity must be held extremely low, with typically one microwave photon in the cavity on average. This leads to an extremely weak transmitted signal of about 100 attowatts (10^{-16} W) which is amplified by a quantum-limited microwave amplifier developed in-house at the Institut Néel. We have succeeded in continuously monitoring the state of the qubit in real time, demonstrating a high level of non-destructive quantum measurement, see Fig. 2.

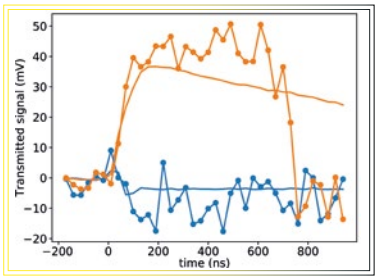

Fig. 2: The data points are two continuous measurements in real time of the state of the qubit, after the qubit had been prepared in its ground state $|g\rangle$ (blue) and in its excited state $|e\rangle$ (orange), respectively. The two states $|g\rangle$ and $|e\rangle$ are clearly separated for an integration time as short as 30 nanoseconds. Here we show a measurement that caught a spontaneous quantum jump between the two states, at time t = 750 ns. The blue and red curves are averages over 1000 measurements.

This study enlightens some fundamental aspects of quantum measurements. In addition, improving readout will have a major role in active error-correction for quantum information processing. Our novel cross-Kerr coupling method opens new possibilities for circuit quantum-electrodynamics research, and it can be implemented in a multi-qubit platform.

further reading...

- **Fast high fidelity quantum non-demolition qubit readout via a non-perturbative cross-Kerr coupling**
  R. Dassonneville, T. Ramos, V. Milchakov, L. Planat, E. Dumur, F. Foroughi, J. Puertas, S. Leger, K. Bharadwaj, J. Delaforce, C. Naud, W. Hasch-Guichard, J.-J. Garcıa-Ripoll, N. Roch & O. Buisson. *Phys. Rev.* X 10, 011045 (2020).
- **Understanding the saturation power of Josephson parametric amplifiers made from SQUID arrays**
  L. Planat, R. Dassonneville, J. Puertas-Martinez, F. Foroughi, O. Buisson, W. Hasch-Guichard, C. Naud, R. Vijay, K. Murch & N. Roch. *Phys. Rev. Appl.* 11, 034014 (2019).

Contacts
olivier.buisson@neel.cnrs.fr • nicolas.roch@neel.cnrs.fr

PhD students
Rémy Dassonneville • Vladimir Milchakov
Luca Planat

A new topological phase in graphene

Topological insulators form a new class of materials of great interest for quantum technologies. By playing with the electronic properties of graphene in a novel way, we have succeeded in fabricating a new topological phase for graphene, thus combining the qualities of graphene and those of topological insulators.

Graphene, a 2-D material, a single layer of carbon atoms, is a conductive material with multiple advantages for new technologies. When a graphene sheet is subjected to an intense magnetic field perpendicular to its plane, a quantum Hall effect occurs, localizing electrons in the bulk of the graphene and creating one dimensional conductive channels propagating along the two edges of the graphene flake.

The quantum Hall effect is specific to 2-D materials and is explained by the way in which the Landau levels (energy levels associated with the spinning motion of the electrons around an applied magnetic field) are positioned in the band structure. Remarkably, in graphene, this effect exists even at room temperature. There is another effect, the "quantum spin-Hall" effect, generally obtained at very low temperature, in which the magnetic field is replaced by the spin-orbit coupling (between an electron's spin and its orbital motion) and the electrical charges appearing at the edges become spin-polarized. Theory predicts that the graphene sheet then becomes a "topological insulator", conductive only at its edges. This topological phase predicted with the quantum spin-Hall effect had not been observed for graphene so far.

At the Institut Néel, using a radically new approach, in collaboration with the National Laboratory for Intense Magnetic Fields (LNCMI-Grenoble) and with Chinese and Japanese researchers, we have created this topological phase of graphene. We started from the quantum Hall effect and sought to control the Coulomb interactions by coupling a graphene sheet with a strontium titanate ($SrTiO_3$) substrate, which has dielectric constant ≈ 10 000. This new phase is extremely robust, requires only moderate magnetic fields, and is stable up to 110 Kelvin.

The graphene and the $SrTiO_3$ substrate are separated by a thin layer of hexagonal boron nitride (h-BN), see Fig. 1. This controls the Landau levels band structure: coulomb interactions between the graphene's electrons are screened by the substrate. For small thicknesses of the h-BN layer (<10 nm), a spin separation appears in the Landau levels which gives the graphene the same properties as those of the quantum spin Hall effect. A pair of 1-D conduction channels of opposite spins then appears on each edge of the sheet (Fig. 2). This is a helical arrangement, insofar as the spin direction is related to that of the electron propagation. This property limits the diffusion of electrons from one channel to the other and confers the properties of quantum coherence to the topological state.

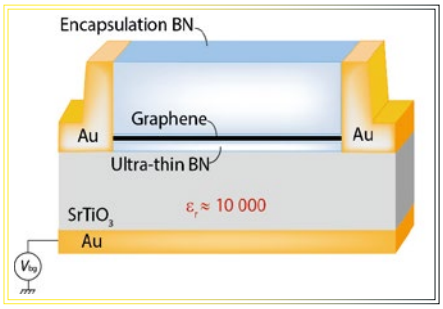

Fig. 1: The graphene sample encapsulated between two flakes of boron nitride (BN) and deposited on a strontium titanate ($SrTiO_3$) substrate.

Our work required exact positioning of an extremely thin and pure layer of h-BN between the graphene and the $SrTiO_3$ substrate in order to benefit from the screening and to control coulomb interactions. Due to its relative simplicity of manufacture and its compatibility with magnetic or superconducting materials, this topological phase of graphene has considerable application prospects. By coupling it to superconducting electrodes, it could, for example, allow the fabrication of protected quantum states, the fermions of Majorana, usable for future generations of quantum computers.

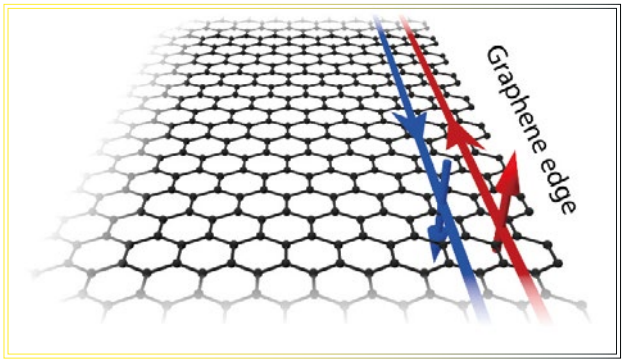

Fig. 2: The graphene sheet and the two conducting edge-channels in the new topological phase. A pair of helical conduction channels propagate in opposite directions along the graphene's edges. Red and blue arrows perpendicular to the graphene represent the two spin orientations (up and down). The arrows in the plane represent the two electron-propagation directions.

further reading...

- **Helical quantum Hall phase in graphene on $SrTiO_3$**
  L. Veyrat, C. Déprez, A. Coissard, Xiaoxi Li, F. Gay, Kenji Watanabe, Takashi Taniguchi, Zheng Han, B.-A. Piot, H. Sellier & B. Sacépé
  Science 367, 781 (2020).

Contact
benjamin.sacepe@neel.cnrs.fr

Director of publication:
Étienne Bustarret
Editors:
Ronald Cox, Jan Vogel
Production manager:
Nathalie Bourgeat-Lami
Layout:
Florence Fernandez, Anne-Laure Jaussent
Printing:
Press'Vercors
December 2020

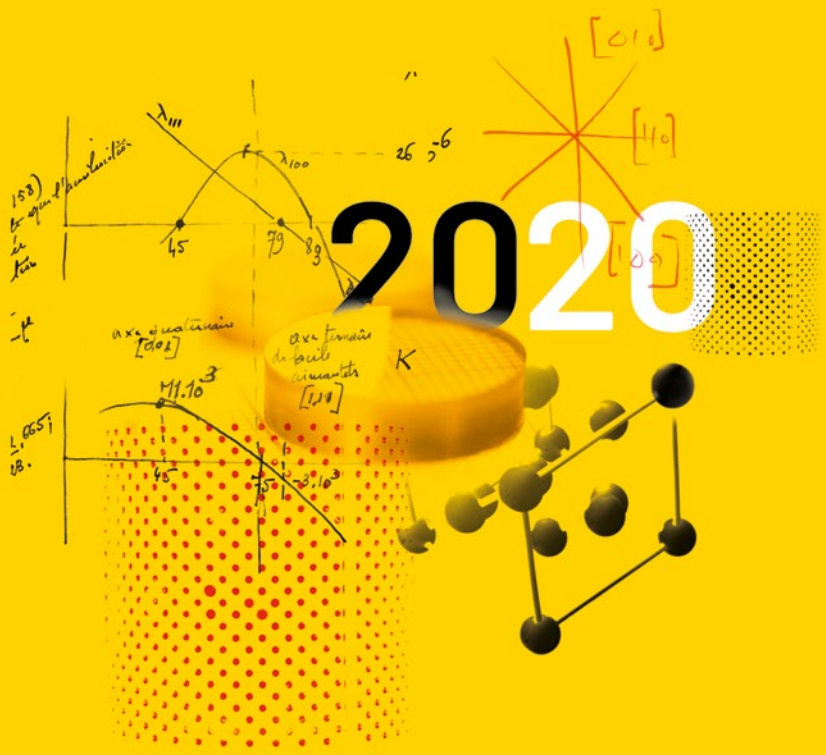

Highlights

20 n°14

Institut Néel - CNRS
25, rue des Martyrs - BP166
38042 Grenoble cedex 9 - France

neel.cnrs.fr